Colistin-loaded aerosolizable particles for the treatment of bacterial respiratory infections

Guillermo Landa[a,b,c†], Teresa Alejo[a,b,c†], Theo Sauzet[d], Victor Sebastian[a,b,c], Frederic Tewes[*,d], Manuel Arruebo[a,b,c]

[a]Instituto de Nanociencia y Materiales de Aragon (INMA), CSIC-Universidad de Zaragoza, Zaragoza 50009, Spain

[b]Department of Chemical Engineering. University of Zaragoza, Campus Río Ebro-Edificio I+D, C/ Poeta Mariano Esquillor S/N, 50018 Zaragoza, Spain

[c]Networking Research Center on Bioengineering, Biomaterials and Nanomedicine, CIBER-BBN, 28029-Madrid, Spain

[d] Université de Poitiers, INSERM U1070, Poitiers, France

[*]Corresponding author: FT: ftewes@univ-poitiers.fr

[†]GL and TA: both authors contributed equally to this manuscript.

ABSTRACT

Compared to parenteral administration of colistin, its direct pulmonary administration can maximize lung drug deposition while reducing systemic adverse side effects and derived nephrotoxicity. Current pulmonary administration of colistin is carried out by the aerosolization of a prodrug, colistin methanesulfonate (CMS), which must be hydrolized to colistin in the lung to produce its bactericidal effect. However, this conversion is slow relative to the rate of absorption of CMS, and thus only 1.4% (w/w) of the CMS dose is converted to colistin in the lungs of patients receiving inhaled CMS. We synthesized several aerosolizable nanoparticle carriers loaded with colistin using different techniques and selected particles with sufficient drug loading and adequate aerodynamic behavior to

efficiently deliver colistin to the entire lung parenchyma. Specifically, we carried out i) the encapsulation of colistin by single emulsion-solvent evaporation with immiscible solvents using polylactic-co-glycolic (PLGA) nanoparticles; ii) its encapsulation using nanoprecipitation with miscible solvents with poly(lactide-co-glycolide)-block-poly(ethylene glycol) as encapsulating matrix; iii) colistin nanoprecipitation using the antisolvent precipitation method and its subsequent encapsulation within PLGA nanoparticles; and iv) colistin encapsulation within PLGA-based microparticles using electrospraying. Nanoprecipitation of pure colistin using antisolvent precipitation showed the highest drug loading (55.0 ± 4.8 wt.%) and spontaneously formed aggregates with adequate aerodynamic diameter (between 3 to 5 μm) to reach the entire lung. These nanoparticles were able to inhibit the growth of *Pseudomonas aeruginosa* in an *in vitro* model of lung biofilm infection at 5 μg/ml (MIC), while completely eradicating the bacteria at 10 μg/ml (MBC). This formulation could be a promising alternative for the treatment of pulmonary infections improving lung deposition and, therefore, the efficacy of aerosolized antibiotics.

KEYWORDS: polymeric nanoparticles; PLGA; colistin; antimicrobial effect; aerosol; pulmonary delivery; *Pseudomonas aeruginosa.*

INTRODUCTION

Colistin (polymyxin E) is a polypeptide antibiotic of last resort, which is normally used in combination with other antibiotics in the treatment of multidrug-resistant (MDR) and extensively drug-resistant (XDR) Gram-negative infections (Ahn et al., 2017). Colistin binds to lipid A of the outer membrane lipopolysaccharides (OM) of Gram-negative bacteria, then disrupts the OM and inner membrane and causes cell lysis. To reduce its

neuro- and nephrotoxicity, colistin is administered as the prodrug colistin sodium methanesulfonate (CMS), which is hydrolyzed after parenteral administration or after inhalation releasing its active form (i.e., colistin). However, intravenous (IV) colistin shows limited pulmonary diffusion and has a significant nephrotoxicity (Rello et al., 2017). Nowadays, CMS is administered by the pulmonary route as a powder, in PEG-gelatin capsules (Colobreathe®), or as solutions using nebulizers (eFlow® rapid, PARI LC PLUS®), to treat chronic pulmonary infections caused by *Pseudomonas Aeruginosa* in patients with cystic fibrosis (Schuster et al., 2013).

However, CMS is not an optimal prodrug. In fact, CMS is inactive against *P. aeruginosa* and has to be converted by non-enzymatic hydrolysis into colistin to produce its bactericidal effect (Bergen et al., 2006). This conversion is slow compared to the CMS pulmonary absorption rate (Boisson et al., 2017, 2014; Couet et al., 2012). In addition, in critically ill patients receiving CMS by nebulization, only 1.4% (w/w) of the CMS dose is converted into colistin in the lung (Boisson et al., 2014). Therefore, relatively high CMS concentrations are required to obtain effective colistin concentrations in the pulmonary epithelial lining fluid (ELF). Still, the International Consensus Guidelines for the Optimal Use of the Polymyxins, endorsed by the American College of Clinical Pharmacy, the European Society of Clinical Microbiology and Infectious Diseases, the Infectious Diseases Society of America, the International Society for Anti-infective Pharmacology, the Society of Critical Care Medicine, and the Society of Infectious Diseases Pharmacists indicate that despite the risks associated to the use of nebulized colistin its potential benefits outweigh them due to a reduced associated nephrotoxicity and increased concentration of the drug in the lung parenchyma; although those professional associations indicate that more randomized clinical trials are needed to draw solid conclusions (Tsuji et al., 2019). Therefore, site-specific drug delivery systems for

the efficient pulmonary delivery of colistin can increase the antibiotic local concentration while avoiding unwanted side effects making them adequate even for patients with other underlying pulmonary conditions.

The “respirable mass” (mass that is deposited on the lung parenchyma by gravitational sedimentation) is maximum for particles having a mass median aerodynamic diameter between 1 and 5 μm. Larger particles are retained by inertial impaction or interception in the upper airways (i.e., oropharyngeal deposition) and smaller particles remain suspended for prolonged periods of time by diffusion being a large fraction exhaled. Alveolar deposition is then maximum for those particle sizes in the 1 to 5 μm range and also for submicron particles (<100nm) (Kodros et al., 2018) but it is complex to maintain a stable aerosol having submicron sizes, mainly because of their high surface reactivity and tendency to agglomeration.

Different strategies have been followed in order to maximize drug accumulation in the lung parenchyma when treating respiratory infections. Drug particle sizes have been tuned in order to maximize deposition and avoiding exhalation in this targeted micron size (Miller et al., 2021). Also, thiolated drug delivery vehicles (e.g., polymers), commonly named thiomers, have been extensively used in pulmonary drug delivery to promote antibiotic-loaded carrier mucoadhesion while avoiding mucus turn over due to their ability to form disulfide bonds with the cysteine-rich subdomains of lung mucus glycoproteins via thiol-disulfide exchange reactions (Dünnhaupt et al., 2015). Hydrophobic interactions between most of the hydrophobic polymers used are also responsible for the observed mucoadhesion (Nafee et al., 2014). PEGylation is also a common strategy to either promote mucoadhesion or mucus-penetrating ability depending on its structure (i.e., linear, brush) and molecular weight, avoiding, at the same time, mucociliary clearance. PEG mucoadhesion ability has been attributed to the

hydrogen bonding of the two lone electron pairs of oxygen in PEG repeat unit with mucin (Guichard et al., 2017). Its mucus-penetrating ability has been attributed to the neutral hydrophilic character and steric hindrance of high-density low molecular weight PEGs functionalizing drug-loaded nanoparticles which avoid particle agglomeration or irreversible aggregation. PEGylation on polymer nanoparticles improves lung retention and drug availability due to its rapid diffusion through the mucus layer reaching the underlying epithelial cells (Schneider et al., 2017).

The aliphatic polyester polylactic-co-glycolic acid (PLGA) is one of the most frequently used polymers for the sustained delivery of antibiotics due to its hydrolytic nature which makes it to decompose in biodegradable endogenous lactic and glycolic acids. Its molecular weight and the molar ratio of the monomers present can be tuned to provide with different degradation half-lives and the consequent specific release kinetics. Aerosolizable colistin has been previously encapsulated within PLGA showing prolonged antibiofilm action against biofilm-forming *P. aeruginosa* ATCC 27853 with just one single application compared to the multiple treatments required to exert the same antimicrobial action when using the free antimicrobial peptide (d'Angelo et al., 2015b). However, colistin loadings achieved using this single emulsion solvent evaporation synthesis technique were not very high (i.e., 1.27 wt.%) (d'Angelo et al., 2015b). Other works using a similar approach for the formation of colistin loaded PLGA microparticles also rendered moderate drug loadings < 5wt.% (Nanjo et al., 2013). Using double emulsion solvent evaporation Shi *et al.* (Shi et al., 2010) encapsulated colistin sulfate salt in PLGA microparticles having drug loadings up to 16 wt.%. Despite all these efforts, it has not yet been possible to obtain high drug loadings of more than 50 wt% in PLGA micro- and nanoparticles with hydrodynamic sizes suitable for pulmonary delivery. Herein, we propose the encapsulation of colistin in PLGA nanoparticles intended for

pulmonary delivery using: i) single emulsion-solvent evaporation; ii) nanopreciptation using miscible solvents with PLGA-PEG, poly(lactide-co-glycolide)-block-poly(ethylene glycol), as encapsulating matrix; iii) colistin nanoprecipitation using the antisolvent precipitation method to render nanoparticles used either standing-alone or encapsulated within PLGA nanoparticles; and iv) colistin encapsulation within PLGA-based microparticles using electrospraying.

EXPERIMENTAL SECTION

Materials and methods

Hydroxypropyl methylcellulose (HPMC, Mn ~10,000), poly(ethylene glycol) (PEG300, Mn 300), Pluronic® F68 (average Mw 8350 Da), poly(ethylene glycol) methyl ether-block-poly(lactide-co-glycolide) (PEG-PLGA, PEG average Mn 5,000, PLGA Mn 25,000, lactide:glycolide 50:50), sodium hydroxide (≥98%), the contrast agent phosphotungstic acid (reagent grade), as well as N,N-dimethylformamide (DMF) and ethyl acetate, used as solvents, were supplied by Sigma-Aldrich. Acros Organics provided the colistin sulfate salt (≥77%). The polymer poly (D,L-lactic acid/glycolic acid) 50/50 ester terminated (PLGA, Mw 38-54 kDa) Resomer® RG 504 was purchased from Evonik Industries AG (Darmstadt, Germany). All of these chemicals were used as received.

Synthetic procedures

Synthesis of hydrophobic unprotonated colistin (colistin base). Colistin sulfate salt was dissolved in Milli-Q water at a final concentration of 20 mg/mL, after its complete dissolution, its hydrophobic form was obtained by adding dropwise a 0.2 M NaOH solution under stirring. The NaOH solution was constantly added until a pH of 11 was obtained because colistin is comprised of five amine groups with an estimated pK_a of ~10 (Ma et al., 2009), and consequently the non-water soluble colistin precipitated as a white

solid. This solid was filtered under vacuum and washed with deionized water several times. The solid was dried under vacuum overnight obtaining a 60 wt.% synthesis yield.

Preparation of colistin nanoparticles (CNPs)- coacervation. Colistin nanoparticles (CNPs) were prepared using the anti-solvent precipitation technique adapted from a previously reported method (Alejo et al., 2021). CNPs prepared using this technique were chosen to increase the drug loading, compared to other synthesis techniques, because they are composed of a large amount of pure drug. With this aim, 15 mg of hydrophobic colistin were incorporated in 1.5 mL of PEG300 by stirring with mild heating. The anti-solvent solution was prepared by adding 100 mg of HPMC in 3.5 mL of water. To allow HPMC dissolution, the water was heated at 80 ºC under stirring until the powder was well dispersed, then, cooled down in an ice bath to solubilize the HPMC. The colistin in PEG300 was quickly added to the HPMC solution under continuous stirring at 400 rpm and room temperature during 2 min. The final organic and aqueous phase ratio was 3/7, where HPMC content was 2% w/w in the final dispersion. After drug solution addition, the solution turned into a stable opaque dispersion indicating the formation of CNPs stabilized with HPMC. To precipitate the CNPs, the final dispersion was centrifuged at 13000 rpm for 30 minutes, then the supernatant was replaced with water and the solid was redispersed. The CNPs were then washed with water to remove the excess of unreacted polymer. Finally, the obtained CNPs were freeze-dried to obtain a white dry powder and stored for further use.

Synthesis of PLGA-colistin nanoparticles (PLGA-col). PLGA-col nanoparticles were prepared using the oil-in-water (o/w) single emulsion solvent evaporation method. Briefly, 50 mg of PLGA polymer, 150 mg of Pluronic-F68 and different amounts of hydrophobic colistin (12.5-50 mg) were dissolved in 5 mL of ethyl acetate. Then, this organic phase was emulsified with 10 mL of Milli-Q water as aqueous phase by

sonication in an ice bath for 25 seconds using an ultrasonic probe of 0.13 inches of diameter and setting an amplitude of 40% (Digital Sonifier 450, Branson, USA). The resulting o/w emulsion was maintained under continuous stirring (600 rpm) during 3 h in order to evaporate the ethyl acetate. The obtained nanoparticles were washed by centrifugation at 7500 rpm for 15 min and lastly dispersed in 2 mL of Milli-Q water before use.

Synthesis of PLGA-PEG-colistin nanoparticles (PLGA-PEG-col). Hydrophobic colistin was encapsulated in PLGA-PEG using the nanoprecipitation method. In this method, 5 mg of PLGA-PEG and different amounts of hydrophobic colistin (2.5-9 mg) were dispersed in 1 mL of acetone. This dispersion was dropwise added at a flow rate of 2 mL/h using a syringe pump (model PHD Ultra, Harvard Apparatus, Holliston, MA, USA) over 1 mL of Milli-Q water under constant magnetic stirring. When the addition was completed, the acetone was evaporated by stirring at room temperature for 2 hours to induce the precipitation of the polymer nanoparticles. The resulting PLGA-PEG-colistin nanoparticles were purified by centrifugation and washing with Milli-Q water (10000 rpm/10 min).

PLGA-colistin microparticles (PLGA-col MPs) electrospraying. PLGA-col microparticles were prepared by electrospray using an Yflow 2.2 D500 electrospinner (Electrospinning Machines/R&D Microencap-sulation, Valencia, Spain) equipped with an 8 cm diameter aluminum disc plate covered with an aluminum foil as collector, as previously reported (Gámez-Herrera et al., 2020). A dispersion of PLGA (10% w/w) and hydrophobic colistin in DMF containing different amounts of colistin (10, 15, 20, 30 wt.% referred to the polymer mass) was prepared by stirring the solution overnight at room temperature. The PLGA-col mixture was loaded into a 10 mL syringe and supplied to the electrospinner nozzle using a syringe pump connected to a 22-gauge needle that

functioned as the spraying nozzle and positioned at 30 cm from the collector plate in order to efficiently evaporate the DMF solvent during the electrospraying process. The flow rate was set at 0.5 mL/h and the applied voltage at -3.80 kV for the collector, and between + 10.0 kV and +14.5 kV for the needle, obtaining a stable Taylor cone-jet. Digital visualization of the spraying process was performed through a video camera. The microparticles were obtained at room temperature and a relative humidity between 30% and 50%. The resulting microparticles were obtained as a white dry powder by gently scratching the aluminum foil with a spatula.

Nanoparticle characterization

The hydrodynamic size of the resulting nanoparticles was measured using dynamic light scattering (DLS) in a Brookhaven 90Plus particle size analyzer with a detection angle of 90º. Measurements were taken at 25 ºC ± 0.1 ºC. Zeta potential measurements were performed on a Brookhaven 90Plus particle size analyzer using the ZetaPALS software in 1 mM KCl aqueous solution at a pH = 6 and 25 ± 0.1 ºC. The zeta potential was determined by studying their electrophoretic mobility and then applying the Smoluchowski equation.

Transmission electron microscopy (TEM) images were recorded in a T20-FEI Tecnai thermionic microscope operated at an acceleration voltage of 200 kV. Samples were dropped on carbon coated copper grids, dried at room temperature and stained with a negative staining agent (3% phosphotungstic acid) to improve the contrast of the polymeric nanoparticles. Morphological characterization of the NPs was also performed using an Inspect F-50 Scanning Electron Microscope, (SEM FEI, Holland), with the NPs previously coated with a palladium layer. Microscopy images were analyzed using the open source image processing software ImageJ to obtain the corresponding particle size distribution histograms.

Aerodynamic particle diameter analysis

The aerodynamic particle size distribution of CNPs and PLGA MPs was studied using a Next Generation Impactor (NGI, Copley Scientific Limited, Nottingham, UK), equipped with a TPK 2000 critical flow controller and a HCP5 vacuum pump (Copley HCP5, Nottingham, UK). The flow rate was adjusted to get a pressure drop of 4 kPa in the powder inhaler (Handihaler®, Boeringher, Ingelheim, Germany), and the time of aspiration was adjusted to obtain 4 L of air. For each test (N=3), the inhaler was loaded with a size 3 hard gelatin capsule filled with 21 ± 1 mg of the corresponding dry particles. Then, two cycles of aspiration were carried out. After the particles were emitted, the particles staying in the capsule, in the inhaler, and deposited in the induction port and all the stages of the NGI were recovered. The mass of particles with aerodynamic diameter less than 5 µm, expressed as a percentage of the total mass emitted and recovered, was considered the fine particle fraction (FPF). The mass median aerodynamic diameter (MMAD) and FPF were calculated as previously described (Gaspar et al., 2015; Lamy et al., 2019, 2018; Tewes et al., 2020). Particles with aerodynamic diameters between 3 and 5 µm were collected and used for colistin release studies.

Colistin loading and *in vitro* release

For the evaluation of *in vitro* drug release kinetics, 2 mg of CNPs particles with an aerodynamic diameter between 3-5 µm were dispersed in 12 mL of ammonium acetate buffer (0.1 M, pH 7). Aliquots of this suspension were placed in tubes and incubated for 24 hours. (37 ºC, 120 rpm). At predetermined time points, tubes (N=3 per time point) were centrifuged at 13.000 rpm for 5 min (Eppendorf centrifuge 5418R) and supernatants were collected. The colistin concentration in the samples was determined by a validated LC-MS/MS method as previously described (Gobin et al., 2010; Marchand et al., 2010; Gontijo et al., 2014; Boisson et al., 2014, 2017; Tewes et al., 2020). Briefly, the

chromatography was performed on an Alliance 2695 system (Waters, France) with a Jupiter 300-Å column (5.0 µm, 50mm, 2.0-mm i.d.; Waters, St.-Quentin en Yvelines, France) and a mobile phase (flow rate 0.2 mL/min) consisting of 0.1% (v/v) formic acid in acetonitrile – 0.1 % (v/v) formic acid in water (25:75 v/v). The mass spectrometer Micromass Quattro microAPI (Waters, France) was used in the positive/ion mode. The calibration standard curve was prepared with seven samples in ammonium acetate buffer with colistin base concentrations ranging between 0.01 and 10 $\mu g \cdot mL^{-1}$.

To measure the colistin loading and encapsulation efficiencies of the different synthesized particles, liquid/liquid extractions of the PLGA or PLGA-PEG polymers were performed using a 1:1 (v/v) mixture of methylene chloride/0.1% (v/v) formic acid in water. For CNPs, complete dissolution of colistin in 0.1% (v/v) formic acid in water was performed for 24 hours. Then, a similar LC-MS/MS method was used to assay colistin in the 0.1% (v/v) formic acid in water phase. Controls made of a known amount of colistin showed 100% recovery of colistin in both cases. The encapsulation efficiency (EE) and the drug loading (DL) were calculated with eqn. 1 and 2, respectively:

$$EE\ (\%) = \frac{mass\ of\ entrapped\ colistin\ (mg)}{mass\ of\ colistin\ added\ (mg)}\ x\ 100 \quad (1)$$

$$DL\ (\%) = \frac{mass\ of\ entrapped\ colistin\ (mg)}{Total\ mass\ of\ colistin\ loaded\ particles\ (mg)}\ x\ 100 \quad (2)$$

Microbiological studies

P. aeruginosa loaded alginate beads preparation. Pseudomonas aeruginosa PAO1 strain made bioluminescent by chromosomal integration of the luxCDABE operon was provided by Professor Patrick Plesiat (Centre National de Référence de la résistance aux antibiotiques, Centre Hospitalier Universitaire de Besançon, France). Mueller-Hinton Broth (MHB), parafilm oil, sorbitan monooleate (SPAN®60), Trizma® hydrochloride (TRIS-HCL) and calcium chloride were purchased from Sigma Aldrich, France.

Alginate beads loaded with PAO1 were prepared according to the method described by Torres *et al.* (Torres et al., 2019). PAO1 cultures in MHB were incubated to reach exponential growth phase and then diluted to an OD_{600} of 0.3. One mL of this suspension was washed by centrifugation with 0.9 % (w/v) NaCl and then dispersed in 9 mL of 2 % (w/v) alginate. Then, this preparation was emulsified with 100 mL of paraffin oil containing 0.01 % (v/v) of SPAN®60 using a mechanical stirrer (RZR-2021, Heidolph, France) at 1300 rpm. For the gelation of the droplets containing the alginate, 20 mL of 0.1 M TRIS-HCl buffer pH 7 containing 0.1 M of $CaCl_2$ were added dropwise to the emulsion and kept under stirring. Finally, the emulsion was allowed to cool for 1 hour by putting an ice bath around the beaker under moderate stirring (300 rpm). After the formation, the alginate beads were centrifuged at 5000g for 10 min and washed 4 times with 0.9% (w/v) NaCl.

Antimicrobial activity of CNPs. Mueller-Hinton agar (MHA), colistin sulfate salt, sodium citrate dihydrate and sodium bicarbonate were purchased from Sigma Aldrich, France. Freshly prepared alginate beads loaded with PAO1 were dispersed in 5 mL of Mueller-Hinton broth (MHB). Then, 100 µL of the suspension was dispensed in each well of white, flat-bottomed 96-well microplates (Greiner®, France). The bioluminescence of the wells was recorded over time until an intensity of ≈1000 RLU was achieved. At that moment, 100 µL of MHB solutions with increasing concentrations of colistin and CNPs (from 0.2 to 40 µg/mL). Then, the plates were sealed with a clear membrane to prevent evaporation and luminescence was recorded every 30 min for 24 h at 37 °C using a microplate reader (Infinite 200 Pro, Tecan, France). After 24h, in order to release the bacteria from the alginate beads, cultures were diluted in a citrate - bicarbonate buffer (0.02 M citric acid, 0.05 M Na_2CO_3) and incubated 10 min at 37 °C in an orbital shaker

(200 rpm). Solubilized beads were then serially diluted in 0.9 % (w/v) NaCl and plated on MHA plates for bacterial count by colony formation.

RESULTS

Preparation and characterization of colistin-loaded nano and microparticles

In this work, several different polymeric nano- and microparticles have been developed for the encapsulation of colistin. Depending on the particle size desired, and in order to achieve high drug loadings, different fabrication techniques were used to obtain the desired colistin-loaded particles; namely, o/w emulsification, nanoprecipitation, complex coacervation, and electrospraying.

The oil-in-water (o/w) single emulsion solvent evaporation method was successfully used for preparing PLGA-col nanoparticles. The amount of hydrophobic colistin added to the emulsion was varied to explore the optimal amount for an improved drug loading. Figure 1a depicts a representative SEM image of the resulting PLGA-col nanoparticles prepared using 50 mg of hydrophobic colistin in the synthesis. SEM and TEM images of the nanoparticles obtained using 12.5 and 30 mg of hydrophobic colistin are presented in Fig S1. The resulting PLGA nanoparticles exhibited the characteristic spherical shape, and the particle size distribution histogram obtained from the SEM images showed that narrow particle size distributions were achieved, resulting in a mean diameter value of 113 ± 31 nm (when using 12.5 mg of colistin in the synthesis), 118 ± 34 nm (when using 30 mg of colistin in the synthesis), and 105 ± 28 nm (when using 50 mg of colistin in the synthesis) (Figure 1 and Figure 1S). The size and shape of the polymeric nanoparticles were not significantly affected by the amount of drug incorporated during the synthesis. TEM images of stained PLGA-col nanoparticles (Figure 1b) exhibited spherical monodisperse nanoparticles. Furthermore, it is possible to observe dark grey regions located inside the particles that are more noticeable in the samples with the highest

concentration of colistin used (Fig. 1b), which can be ascribed to the presence of colistin inside them and that is also stained by the contrast agent used to improve electron microscopy imaging. When the nanoparticles were incubated in an aqueous medium with a pH adjusted to 6-7 those grey areas disappeared in the TEM images (Figure 1c), probably due to the solubilization and release of the encapsulated colistin. This can be explained by the fact that colistin is positively charged at neutral pH due to the presence of amine functional groups in its structure and becomes soluble in water (Dubashynskaya and Skorik, 2020). The hydrodynamic size of PLGA-col nanoparticles with 50 mg of colistin used during their synthesis determined by DLS was 300 ± 60 nm. Table 1 shows that the colistin loading using this technique was less than 2 wt.% (1.8 ± 0.6 wt.%).

As described in the introduction section the surface modification using specific polyethylene glycols (PEGs) can increase the pulmonary biodistribution of drug-loaded nanoparticles, protects nanocarriers from the immune system, and also enhances the mucopenetration of nanoparticles administrated through the nasal and pulmonary routes when forming inhalation aerosols (Muralidharan et al., 2014). Therefore, colistin-loaded PLGA-PEG nanoparticles were prepared using the nanoprecipitation method as described above. Different concentrations of colistin in the organic phase (2.5, 5, 7, and 9 mg/mL) were evaluated. Representative histograms and SEM images of the nanoparticles obtained are shown in Fig 1e, 1f and Fig S2, exhibiting nanoparticle mean sizes centered at 77 nm, which are slightly smaller than the size of PLGA nanoparticles obtained using the emulsification method (Fig. 1d). TEM images (Fig 1g and Fig S2) also showed the formation of PLGA-PEG-colistin nanoparticles at different colistin concentrations. Table 1 shows that the colistin loading using this technique was 5.3 wt.% ± 2.9. The hydrodynamic size, determined by DLS, of those PLGA-PEG-colistin nanoparticles

having the highest loading was 424 ± 55 nm, which may indicate that colistin induced incipient nanoparticle agglomeration.

A different approach was also explored to improve drug loading in the nanocarriers, by nano-coacervation of hydrophobic colistin. By changing the size of the drug crystals to the nanosize range, the specific surface area is increased and, consequently, it is possible to obtain nanomaterials with high drug loadings being efficient drug delivery systems (Mohammad et al., 2019). The amount of colistin added to the synthesis was optimized using different concentrations ranging from 4.2 to 15 mg (Fig. S3), finding the best results when 15 mg of colistin were used (Fig. 2a and 2b). TEM images in Fig. 2a-c revealed the formation of spherical CNPs with a mean diameter size of 20.5 ± 3.1 nm (N= 100) obtaining a monodisperse particle size distribution. The hydrodynamic size of colloidal dispersions based on CNPs measured by DLS was 415 nm. The zeta potential value obtained for CNPs was +1.71 ± 0.25 mV at pH = 6, close to the isoelectric point, which could explain the agglomeration of CNPs observed by DLS. Table 1 shows that the colistin loading using this technique reached 55.0 wt.%. Those resulting CNPs were also encapsulated within PLGA by the oil-in-water (o/w) single emulsion solvent evaporation method in order to prepare PLGA nanoparticles loaded with separately prepared CNPs. For that purpose, 100 mg of CNPs separately prepared were dispersed in ethyl acetate and emulsified following the same protocol described above. Results showed monodisperse PLGA nanoparticles of 114 nm in size loaded with CNPs (Figure S4). However, the drug loading obtained (1.1 wt.% ± 0.1) was not much higher than that obtained by encapsulating free colistin instead of nanoparticles (see Table 1). This is probably attributed to the loss of the CNPs during the solvent evaporation stage.

Finally, in order to obtain particles in the microscale range, the preparation of PLGA microparticles loaded with colistin was explored using the electrospraying technique. An

initial battery of colistin concentrations were screened in the polymeric precursor solution, in order to obtain optimal DLs and reduced particle polydispersity. Figures 2d-e depict SEM images and size distribution histograms of PLGA-col microparticles fabricated by electrospraying using PLGA 10 % (w/w) and colistin sulfate 20 wt.% (referred to the PLGA mass) in DMF. The particles showed a monodisperse size distribution centered at 1.9 ± 0.3 µm (Figure 2f) which would be potentially adequate for pulmonary delivery.

The drug loading and encapsulation efficiency of the different optimized formulations were analyzed by LC-MS/MS. Results are summarized in Table 1, where it can be seen that the highest loading values were achieved for the nanoparticles of colistin obtained by nano-coacervation of hydrophobic colistin comprising of a 55.0 wt. % of drug. PLGA-MPs obtained by electrospraying showed higher colistin loadings compared to the ones retrieved for PLGA NPs obtained by nanoprecipitation and by o/w emulsification. The drug contents achieved for electrosprayed microparticles (15 wt. %) are in accordance with previous values found for this technique (Aragón et al., 2019; Yus et al., 2020). In addition, the drug loadings obtained for PLGA-col and PLGA-PEG-colistin nanoparticles were similar to those previously reported in the literature when using PLGA (Andreu et al., 2019; Gheffar et al., 2021).

Table 1. Size, drug loading and encapsulation efficiency parameters of the different formulations prepared

	PLGA-col NPs (o/w emulsion) with free colistin	PLGA-col NPs (o/w emulsion) with CNPs	PLGA-PEG-col NPs (nanoprecipitation)	PLGA-col MPs (Electrospraying)	CNPs
Size/nm	105 ± 28	114 ± 27	77 ± 20	1900 ± 300	20.5 ± 3.1
DL%	1.8 ± 0.6	1.1 ± 0.1	5.3 ± 2.9	15 ± 4	55.0 ± 5.0
EE%	9.0 ± 3.0	1.5 ± 0.1	8.3 ± 4.5	75 ± 20	26 ± 5

Considering that the highest drug loading values were obtained using the electrospraying technique and by nano-coacervation of colistin, we selected both formulations for their subsequent evaluation of the aerodynamic particle diameter using a Next Generation Impactor (NGI) for classifying aerosol particle into size fractions. As previously stated, in order to achieve optimal lung deposition, the aerodynamic size of particles intended for inhalation should be between 1 and 5 μm (Edwards et al., 1997; Malamatari et al., 2020).

During the aerosolization process in the NGI, most of the electrosprayed colistin-loaded PLGA microparticles remained deposited in the induction port, indicating that they form aerosols of large aerodynamic sizes that are not suitable for pulmonary delivery. On the contrary, the aerodynamic properties retrieved in the NGI for the CNPs (Figure 3) demonstrated that this formulation is adequate for pulmonary inhalation, showing a mass median aerodynamic diameter (MMAD) of 3.3 ± 0.2 μm and a geometric standard deviation (GSD) of 2.4 ± 0.2 μm. The reported MMAD is in the range of the breathable fraction of an aerosol (1 to 5 μm) considered suitable for pulmonary drug delivery and typical respiratory treatments (Healy et al., 2014). Particles having a MMAD between 1 and 3 μm show higher deposition in the deep lungs in contrast with particles having a MMAD near 5 μm (Carvalho et al., 2011). The percentage of inhaled fine particle mass (particles having an aerodynamic diameter less than 5 μm) relative to the total mass of

particles in the assay was 32.6 ± 0.3 %. Therefore, the synthesis of CNPs was the one which rendered the highest drug loadings (55.0 ± 5.0 %) and appropriated aerosol sizes for pulmonary delivery because after aerosolization those nanoparticles agglomerated forming particles of micron sizes adequate for achieving large pulmonary deposition. Nanoparticles agglomerate into micro-size particles due to their large surface reactivity prone to form supramolecular interactions and also because atmospheric carbon acts as a binder.

Drug release kinetics for the colistin in the CNPs evaluated in acetate buffer showed an immediate burst release profile of all the colistin content under 10 minutes (results not shown), implying a rapid solubilization of colistin from the HPMC matrix. Thus, upon contact with any solubilizing medium at the appropriate pH, CNPs would release their encapsulated colistin, which is a positive outcome because by preventing having bacteria at sub-MIC concentrations the chances to select antimicrobial-resistant mutants would be reduced.

Antimicrobial activity assays against the biofilm model of *P. aeruginosa* showed that CNPs had an antimicrobial activity slightly superior to that observed for the hydrophilic free drug (colistin sulfate salt) (Figure 4). Considering that the drug loading of colistin in the CNPs was 55.0 wt.%, the bactericidal action of colistin against this bacterial model was enhanced, as it is shown in Table 2.

Table 2. Antimicrobial activity of colistin (free and in CNPs) against PAO1 in alginate-beads biofilm model after 24h

	Colistin sulfate (free)	Unprotonated colistin (in CNPs)
MBC (μg/mL)	10	5.5

DISCUSSION

Pulmonary delivery of antibiotic-loaded nanoparticles has a clear advantage over enteral delivery because first-pass metabolism is avoided and because by adjusting the size and surface characteristics of the particles, it is possible to target the drug to the lung parenchyma, providing localized treatment of pulmonary infections. Here we evaluated different protocols for the synthesis of colistin nanoparticles having high drug loadings and an appropriated particle size for pulmonary delivery. Single emulsion-solvent evaporation of PLGA in immiscible solvents (e.g., ethyl acetate and water) is a reliable synthesis technique commonly used for antibiotics encapsulation. Despite its obvious advantages, such as obtaining a homogeneous particle size and its simplicity, the need to use surfactants and the low drug load are its main drawbacks (d'Angelo et al., 2015a; d'Angelo et al., 2015; Nanjo et al., 2013). Herein, we observed drug loadings ≤ 5wt.% when using single emulsion-solvent evaporation and also by nanoprecipitation. Comparing both techniques a superior colistin encapsulation was observed when using nanoprecipitation probably because, in this technique, drug loss is reduced because the organic solvent rapidly diffuses into the aqueous phase due to its miscibility, precipitating the water-insoluble polymer and entrapping the colistin present. Also, a higher vapor pressure of acetone (231 mmHg at 25ºC) compared to that of ethyl acetate (93 mmHg at 25ºC) would facilitate solvent evaporation for the former and a consequent rapid polymer precipitation and drug entrapment. Drug loss during electrospraying is minimized due to the fast solvent evaporation during the ejection of the dissolved polymer from the needle tip to the collector plate. As shown in Table 1, the encapsulation efficiency obtaining by electrospraying is the second highest of the synthesis techniques tested in this work. Drug loadings as high as 15 wt.% were obtained confirming the cost effectiveness of this technique compared to emulsion or nanoprecipitation-based techniques. Also, this

technique operates at room temperature without the need of preserving the polymer from thermal degradation as in the case of emulsion-based techniques where the high shear stress used in the syntheses requires cooling down the resulting suspensions below the glass transition temperature of the polymer (35.7ºC for the 50:50 PLGA) (In Pyo Park and Jonnalagadda, 2006). However, the electrosprayed-loaded PLGA microparticles remained deposited in the pre-separator and in the first stage of the NGI, reflecting their large aerodynamic sizes probably due to their high aggregation, which makes them unsuitable for pulmonary delivery. In agreement with previous reports, we observed that without the use of dispersion modifiers or specific surface coatings, in dry powder inhalation PLGA formulations, a large amount of the microparticles remained in the capsule and in the inhalation device (Scherließ and Janke, 2021). In our study we did not considered the use of surface or intraparticle modifiers such as plasticizers and anti-tacking agents because those would have jeopardized the drug loading of the final aerosolizable pharmaceutical formulations.

Drug nanoprecipitation allows increased drug loadings when using the anti-solvent precipitation technique. HPMC acts as a growth inhibitor on the surface of the growing drug nuclei. This nutrient diffusion barrier allows controlling the particle size in the nanoscale. Once supersaturation is reached, nucleation starts and depending on the availability of the precursors, particle growth begins. The diffusive barrier that HPMC exerts on the surface of the colistin nanoparticles prevented them from further growing. All in all, colistin nanoparticles composed of 55.0 ± 5.0 % of colistin were obtained following this technique (Table 1). Due to their reduced size the resulting CNPs showed enhanced solubility as it has been reported for other nano-coacervates following the same approach (Alejo et al., 2021).

Colistin is a mixture of molecules that forms amorphous solids with high free energy which makes them easy to be dissolved (Zhou et al., 2016). This fact was corroborated by the drug release kinetics obtained for the CNPs in ammonium acetate pH 7.0 where in the first 10 minutes all the drug present in the CNPs was released and its concentration remained constant in the time span analyzed (10 hours) (results not shown). Although drug delivery systems based on HPMC have been reported to cause a gradual release of the drug over time (Li et al., 2010), the highly water soluble HMPC polymeric matrix at the nanometric scale (20.5 nm) could be the reason for the burst release kinetics observed.

Conclusions

Out of four different synthesis protocols tested to obtain high colistin loadings and appropriated aerodynamic sizes to efficiently reach the lung parenchyma, the nanocoacervation of colistin using the antisolvent precipitation method outperforms the other ones (i.e., single emulsion solvent evaporation, nanoprecipitation and electrospraying). The nanocoacervation of the unprotonated form of colistin within HPMC allows reaching drug loadings as high as 55.0 wt.% ± 5.0 showing a mass median aerodynamic diameter of 3.3 ± 0.2 µm, making them adequate for pulmonary delivery. Compared to the free drug, those particles showed enhanced antimicrobial action in a biofilm model of *Pseudomonas aeruginosa* PAO1 strain.

Acknowledgments

Financial support from the Spanish Ministry of Science and Innovation (grant numbers PID2020-113987RB-I00 and CTQ2017-84473-R and RTI2018-099019-A-I00) is gratefully acknowledged. The regional Governments of Aragon and Nouvelle-Aquitaine (by means of the Order PRE/2106/2017) are also gratefully acknowledged. CIBER-BBN

is an initiative funded by the VI National R&D&i Plan 2008-2011 financed by the Instituto de Salud Carlos III with the assistance of the European Regional Development Fund. Authors also acknowledge the LMA-ELECMI ICTS, for offering access to their instruments and for their expertise.

Conflict of interest

The authors declare no conflicts of interest to disclose.

References

Ahn, J.-M., Kassees, K., Lee, T.-K., Manandhar, B., Yousif, A.M., 2017. 6.03 - Strategy and Tactics for Designing Analogs: Biochemical Characterization of the Large Molecules☆, in: Chackalamannil, S., Rotella, D., Ward, S.E.B.T.-C.M.C.I.I.I. (Eds.), . Elsevier, Oxford, pp. 66–115. https://doi.org/10.1016/B978-0-12-409547-2.12413-8

Alejo, T., Uson, L., Landa, G., Prieto, M., Yus Argón, C., Garcia-Salinas, S., de Miguel, R., Rodríguez-Largo, A., Irusta, S., Sebastian, V., Mendoza, G., Arruebo, M., 2021. Nanogels with High Loading of Anesthetic Nanocrystals for Extended Duration of Sciatic Nerve Block. ACS applied materials & interfaces 13, 17220–17235. https://doi.org/10.1021/acsami.1c00894

Andrade, F.F., Silva, D., Rodrigues, A., Pina-Vaz, C., 2020. Colistin update on its mechanism of action and resistance, present and future challenges. Microorganisms 8, 1–12. https://doi.org/10.3390/microorganisms8111716

Andreu, V., Larrea, A., Rodriguez-Fernandez, P., Alfaro, S., Gracia, B., Lucía, A., Usón, L., Gomez, A.-C., Mendoza, G., Lacoma, A., Dominguez, J., Prat, C., Sebastian, V., Ainsa, J.A., Arruebo, M., 2019. Matryoshka-type gastro-resistant microparticles for the oral treatment of Mycobacterium tuberculosis. Nanomedicine 14, 707–726. https://doi.org/10.2217/nnm-2018-0258

Aragón, J., Feoli, S., Irusta, S., Mendoza, G., 2019. Composite scaffold obtained by electro-hydrodynamic technique for infection prevention and treatment in bone repair. International Journal of Pharmaceutics 557, 162–169. https://doi.org/10.1016/j.ijpharm.2018.12.002

Bergen, P.J., Li, J., Rayner, C.R., Nation, R.L., 2006. Colistin Methanesulfonate Is an Inactive Prodrug of Colistin against Pseudomonas aeruginosa. Antimicrob Agents Chemother 50, 1953–1958. https://doi.org/10.1128/AAC.00035-06

Bernal-Mercado, A.T., Juarez, J., Valdez, M.A., Ayala-Zavala, J.F., Del-Toro-sánchez, C.L., Encinas-Basurto, D., 2022. Hydrophobic Chitosan Nanoparticles Loaded with Carvacrol against Pseudomonas aeruginosa Biofilms. Molecules 27, 1–17. https://doi.org/10.3390/molecules27030699

Boisson, M., Grégoire, N., Cormier, M., Gobin, P., Marchand, S., Couet, W., Mimoz, O., 2017. Pharmacokinetics of nebulized colistin methanesulfonate in critically

ill patients. Journal of Antimicrobial Chemotherapy 72, 2607–2612. https://doi.org/10.1093/jac/dkx167
Boisson, M., Jacobs, M., Grégoire, N., Gobin, P., Marchand, S., Couet, W., Mimoz, O., 2014. Comparison of Intrapulmonary and Systemic Pharmacokinetics of Colistin Methanesulfonate (CMS) and Colistin after Aerosol Delivery and Intravenous Administration of CMS in Critically Ill Patients. Antimicrob Agents Chemother 58, 7331–7339. https://doi.org/10.1128/AAC.03510-14
Carvalho, T.C., Peters, J.I., Williams, R.O., 2011. Influence of particle size on regional lung deposition – What evidence is there? International Journal of Pharmaceutics 406, 1–10. https://doi.org/10.1016/j.ijpharm.2010.12.040
Couet, W., Grégoire, N., Marchand, S., Mimoz, O., 2012. Colistin pharmacokinetics: the fog is lifting. Clinical Microbiology and Infection 18, 30–39. https://doi.org/10.1111/j.1469-0691.2011.03667.x
d'Angelo, I., Quaglia, F., Ungaro, F., 2015a. PLGA carriers for inhalation: where do we stand, where are we headed? Therapeutic Delivery 6, 1139–1144. https://doi.org/10.4155/tde.15.37
d'Angelo, I., Casciaro, B., Miro, A., Quaglia, F., Mangoni, M.L., Ungaro, F., 2015b. Overcoming barriers in Pseudomonas aeruginosa lung infections: Engineered nanoparticles for local delivery of a cationic antimicrobial peptide. Colloids and Surfaces B: Biointerfaces 135, 717–725. https://doi.org/10.1016/j.colsurfb.2015.08.027
D'Angelo, I., Casciaro, B., Miro, A., Quaglia, F., Mangoni, M.L., Ungaro, F., 2015. Overcoming barriers in Pseudomonas aeruginosa lung infections: Engineered nanoparticles for local delivery of a cationic antimicrobial peptide. Colloids and Surfaces B: Biointerfaces 135, 717–725. https://doi.org/10.1016/j.colsurfb.2015.08.027
Dubashynskaya, N. V, Skorik, Y.A., 2020. Polymyxin Delivery Systems: Recent Advances and Challenges. Pharmaceuticals (Basel, Switzerland) 13, 83. https://doi.org/10.3390/ph13050083
Dünnhaupt, S., Kammona, O., Waldner, C., Kiparissides, C., Bernkop-Schnürch, A., 2015. Nano-carrier systems: Strategies to overcome the mucus gel barrier. European Journal of Pharmaceutics and Biopharmaceutics 96, 447–453. https://doi.org/10.1016/j.ejpb.2015.01.022
Edwards, D.A., Hanes, J., Caponetti, G., Hrkach, J., Ben-Jebria, A., Eskew, M.L., Mintzes, J., Deaver, D., Lotan, N., Langer, R., 1997. Large Porous Particles for Pulmonary Drug Delivery. Science 276, 1868–1872. https://doi.org/10.1126/science.276.5320.1868
Gámez-Herrera, E., García-Salinas, S., Salido, S., Sancho-Albero, M., Andreu, V., Pérez, M., Luján, L., Irusta, S., Arruebo, M., Mendoza, G., 2020. Drug-eluting wound dressings having sustained release of antimicrobial compounds. European journal of pharmaceutics and biopharmaceutics : official journal of Arbeitsgemeinschaft fur Pharmazeutische Verfahrenstechnik e.V 152, 327–339. https://doi.org/10.1016/j.ejpb.2020.05.025
Gaspar, M.C., Sousa, J.J.S., Pais, A.A.C.C., Cardoso, O., Murtinho, D., Serra, M.E.S., Tewes, F., Olivier, J.-C., 2015. Optimization of levofloxacin-loaded crosslinked chitosan microspheres for inhaled aerosol therapy. European Journal of Pharmaceutics and Biopharmaceutics 96, 65–75. https://doi.org/10.1016/j.ejpb.2015.07.010
Gheffar, C., Le, H., Jouenne, T., Schaumann, A., Corbière, A., Vaudry, D., LeCerf, D., Karakasyan, C., 2021. Antibacterial Activity of Ciprofloxacin-Loaded

Poly(lactic-co-glycolic acid)-Nanoparticles Against Staphylococcus aureus. Particle & Particle Systems Characterization 38, 2000253. https://doi.org/10.1002/ppsc.202000253

Gobin, P., Lemaître, F., Marchand, S., Couet, W., Olivier, J.-C., 2010. Assay of Colistin and Colistin Methanesulfonate in Plasma and Urine by Liquid Chromatography-Tandem Mass Spectrometry. Antimicrobial Agents and Chemotherapy 54, 1941–1948. https://doi.org/10.1128/AAC.01367-09

Gontijo, A.V.L., Brillault, J., Grégoire, N., Lamarche, I., Gobin, P., Couet, W., Marchand, S., 2014. Biopharmaceutical characterization of nebulized antimicrobial agents in rats: 1. Ciprofloxacin, moxifloxacin, and grepafloxacin. Antimicrobial agents and chemotherapy 58, 3942–3949.

Guichard, M.-J., Leal, T., Vanbever, R., 2017. PEGylation, an approach for improving the pulmonary delivery of biopharmaceuticals. Current Opinion in Colloid & Interface Science 31, 43–50. https://doi.org/10.1016/j.cocis.2017.08.001

Healy, A.M., Amaro, M.I., Paluch, K.J., Tajber, L., 2014. Dry powders for oral inhalation free of lactose carrier particles. Advanced Drug Delivery Reviews 75, 32–52. https://doi.org/10.1016/j.addr.2014.04.005

Hong, W., Zhao, Y., Guo, Y., Huang, C., Qiu, P., Zhu, J., Chu, C., Shi, H., Liu, M., 2018. PEGylated Self-Assembled Nano-Bacitracin A: Probing the Antibacterial Mechanism and Real-Time Tracing of Target Delivery in Vivo. ACS Applied Materials and Interfaces 10, 10688–10705. https://doi.org/10.1021/acsami.8b00135

In Pyo Park, P., Jonnalagadda, S., 2006. Predictors of glass transition in the biodegradable poly-lactide and poly-lactide-co-glycolide polymers. Journal of Applied Polymer Science 100, 1983–1987. https://doi.org/10.1002/app.22135

Jensen, S.K., Thomsen, T.T., Oddo, A., Franzyk, H., Løbner-Olesen, A., Hansen, P.R., 2020. Novel Cyclic Lipopeptide Antibiotics: Effects of Acyl Chain Length and Position. International Journal of Molecular Sciences . https://doi.org/10.3390/ijms21165829

Koch, G., 2017. Medicinal Chemistry. Chimia 71, 643. https://doi.org/10.2307/j.ctvnwc0d0.18

Kodros, J.K., Volckens, J., Jathar, S.H., Pierce, J.R., 2018. Ambient Particulate Matter Size Distributions Drive Regional and Global Variability in Particle Deposition in the Respiratory Tract. GeoHealth 2, 298–312. https://doi.org/10.1029/2018GH000145

Lamy, barbara, Serrano, Dolores Remedios, O'Connell, Peter, Couet, W., Marchand, S., Healy, A.M., Tewes, F., 2019. Use of leucine to improve aerodynamic properties of ciprofloxacin-loaded maltose microparticles for inhalation. European Journal of Pharmaceutical Research 1, 2–11.

Lamy, B., Tewes, F., Serrano, D.R., Lamarche, I., Gobin, P., Couet, W., Healy, A.M., Marchand, S., 2018. New aerosol formulation to control ciprofloxacin pulmonary concentration. Journal of Controlled Release 271, 118–126. https://doi.org/10.1016/j.jconrel.2017.12.021

Li, C.L., Martini, L.G., Ford, J.L., Roberts, M., 2010. The use of hypromellose in oral drug delivery. Journal of Pharmacy and Pharmacology 57, 533–546. https://doi.org/10.1211/0022357055957

Ma, Z., Wang, J., Nation, R.L., Li, J., Turnidge, J.D., Coulthard, K., Milne, R.W., 2009. Renal disposition of colistin in the isolated perfused rat kidney. Antimicrobial agents and chemotherapy 53, 2857–2864. https://doi.org/10.1128/AAC.00030-09

Malamatari, M., Charisi, A., Malamataris, S., Kachrimanis, K., Nikolakakis, I., 2020. Spray Drying for the Preparation of Nanoparticle-Based Drug Formulations as Dry Powders for Inhalation. Processes . https://doi.org/10.3390/pr8070788

Marchand, S., Gobin, P., Brillault, J., Baptista, S., Adier, C., Olivier, J.-C., Mimoz, O., Couet, W., 2010. Aerosol Therapy with Colistin Methanesulfonate: a Biopharmaceutical Issue Illustrated in Rats. Antimicrobial Agents and Chemotherapy 54, 3702–3707. https://doi.org/10.1128/AAC.00411-10

Miller, D.P., Tarara, T.E., Weers, J.G., 2021. Targeting of Inhaled Therapeutics to the Small Airways: Nanoleucine Carrier Formulations. Pharmaceutics 13, 1855. https://doi.org/10.3390/pharmaceutics13111855

Mohammad, I.S., Hu, H., Yin, L., He, W., 2019. Drug nanocrystals: Fabrication methods and promising therapeutic applications. International journal of pharmaceutics 562, 187–202. https://doi.org/10.1016/j.ijpharm.2019.02.045

Muralidharan, P., Mallory, E., Malapit, M., Hayes, D.J., Mansour, H.M., 2014. Inhalable PEGylated Phospholipid Nanocarriers and PEGylated Therapeutics for Respiratory Delivery as Aerosolized Colloidal Dispersions and Dry Powder Inhalers. Pharmaceutics 6, 333–353. https://doi.org/10.3390/pharmaceutics6020333

Nafee, N., Husari, A., Maurer, C.K., Lu, C., Rossi, C.D., Steinbach, A., Hartmann, R.W., Lehr, C.M., Schneider, M., n.d. Antibiotic-free nanotherapeutics: Ultra-small, mucus-penetrating solid lipid nanoparticles enhance the pulmonary delivery and anti-virulence efficacy of novel quorum sensing inhibitors. J. Control. Release 192, 131–140. https://doi.org/10.1016/j.jconrel.2014.06.055.

Nanjo, Y., Ishii, Y., Kimura, S., Fukami, T., Mizoguchi, M., Suzuki, T., Tomono, K., Akasaka, Y., Ishii, T., Takahashi, K., Tateda, K., Yamaguchi, K., 2013. Effects of slow-releasing colistin microspheres on endotoxin-induced sepsis. Journal of Infection and Chemotherapy 19, 683–690. https://doi.org/10.1007/s10156-012-0544-y

Rello, J., Solé-Lleonart, C., Rouby, J.-J., Chastre, J., Blot, S., Poulakou, G., Luyt, C.-E., Riera, J., Palmer, L.B., Pereira, J.M., Felton, T., Dhanani, J., Bassetti, M., Welte, T., Roberts, J.A., 2017. Use of nebulized antimicrobials for the treatment of respiratory infections in invasively mechanically ventilated adults: a position paper from the European Society of Clinical Microbiology and Infectious Diseases. Clinical microbiology and infection : the official publication of the European Society of Clinical Microbiology and Infectious Diseases 23, 629–639. https://doi.org/10.1016/j.cmi.2017.04.011

Scherließ, R., Janke, J., 2021. Preparation of Poly-Lactic-Co-Glycolic Acid Nanoparticles in a Dry Powder Formulation for Pulmonary Antigen Delivery. Pharmaceutics 13, 1196. https://doi.org/10.3390/pharmaceutics13081196

Schneider, C.S., Xu, Q., Boylan, N.J., Chisholm, J., Tang, B.C., Schuster, B.S., Henning, A., Ensign, L.M., Lee, E., Adstamongkonkul, P., Simons, B.W., Wang, S.-Y.S., Gong, X., Yu, T., Boyle, M.P., Suk, J.S., Hanes, J., 2017. Nanoparticles that do not adhere to mucus provide uniform and long-lasting drug delivery to airways following inhalation. Science advances 3, e1601556. https://doi.org/10.1126/sciadv.1601556

Schuster, A., Haliburn, C., Döring, G., Goldman, M.H., 2013. Safety, efficacy and convenience of colistimethate sodium dry powder for inhalation (Colobreathe DPI) in patients with cystic fibrosis: a randomised study. Thorax 68, 344–350. https://doi.org/10.1136/thoraxjnl-2012-202059

Shebl, R.I., Farouk, F., Azzazy, H.M.E.-S., 2017. Effect of Surface Charge and Hydrophobicity Modulation on the Antibacterial and Antibiofilm Potential of Magnetic Iron Nanoparticles. Journal of Nanomaterials 2017, 3528295. https://doi.org/10.1155/2017/3528295

Shi, M., Kretlow, J.D., Nguyen, A., Young, S., Scott Baggett, L., Wong, M.E., Kurtis Kasper, F., Mikos, A.G., 2010. Antibiotic-releasing porous polymethylmethacrylate constructs for osseous space maintenance and infection control. Biomaterials 31, 4146–4156. https://doi.org/10.1016/j.biomaterials.2010.01.112

Tewes, F., Brillault, J., Gregoire, N., Olivier, J.-C., Lamarche, I., Adier, C., Healy, A.-M., Marchand, S., 2020. Comparison between Colistin Sulfate Dry Powder and Solution for Pulmonary Delivery. Pharmaceutics 12, 557. https://doi.org/10.3390/pharmaceutics12060557

Torres, B.G.S., Awad, R., Marchand, S., Couet, W., Tewes, F., 2019. In vitro evaluation of Pseudomonas aeruginosa chronic lung infection models: Are agar and calcium-alginate beads interchangeable? European journal of pharmaceutics and biopharmaceutics : official journal of Arbeitsgemeinschaft fur Pharmazeutische Verfahrenstechnik e.V 143, 35–43. https://doi.org/10.1016/j.ejpb.2019.08.006

Tsuji, B.T., Pogue, J.M., Zavascki, A.P., Paul, M., Daikos, G.L., Forrest, A., Giacobbe, D.R., Viscoli, C., Giamarellou, H., Karaiskos, I., Kaye, D., Mouton, J.W., Tam, V.H., Thamlikitkul, V., Wunderink, R.G., Li, J., Nation, R.L., Kaye, K.S., 2019. International Consensus Guidelines for the Optimal Use of the Polymyxins: Endorsed by the American College of Clinical Pharmacy (ACCP), European Society of Clinical Microbiology and Infectious Diseases (ESCMID), Infectious Diseases Society of America (ID. Pharmacotherapy 39, 10–39. https://doi.org/10.1002/phar.2209

Velkov, T., Roberts, K.D., Thompson, P.E., Li, J., 2016. Polymyxins: a new hope in combating Gram-negative superbugs? Future medicinal chemistry 8, 1017–1025. https://doi.org/10.4155/fmc-2016-0091

Yus, C., Irusta, S., Sebastian, V., Arruebo, M., 2020. Controlling Particle Size and Release Kinetics in the Sustained Delivery of Oral Antibiotics Using pH-Independent Mucoadhesive Polymers. Molecular Pharmaceutics 17, 3314–3327. https://doi.org/10.1021/acs.molpharmaceut.0c00408

Zhou, Q. (Tony), Loh, Z.H., Yu, J., Sun, S., Gengenbach, T., Denman, J.A., Li, J., Chan, H.-K., 2016. How Much Surface Coating of Hydrophobic Azithromycin Is Sufficient to Prevent Moisture-Induced Decrease in Aerosolisation of Hygroscopic Amorphous Colistin Powder? AAPS J 18, 1213–1224. https://doi.org/10.1208/s12248-016-9934-x

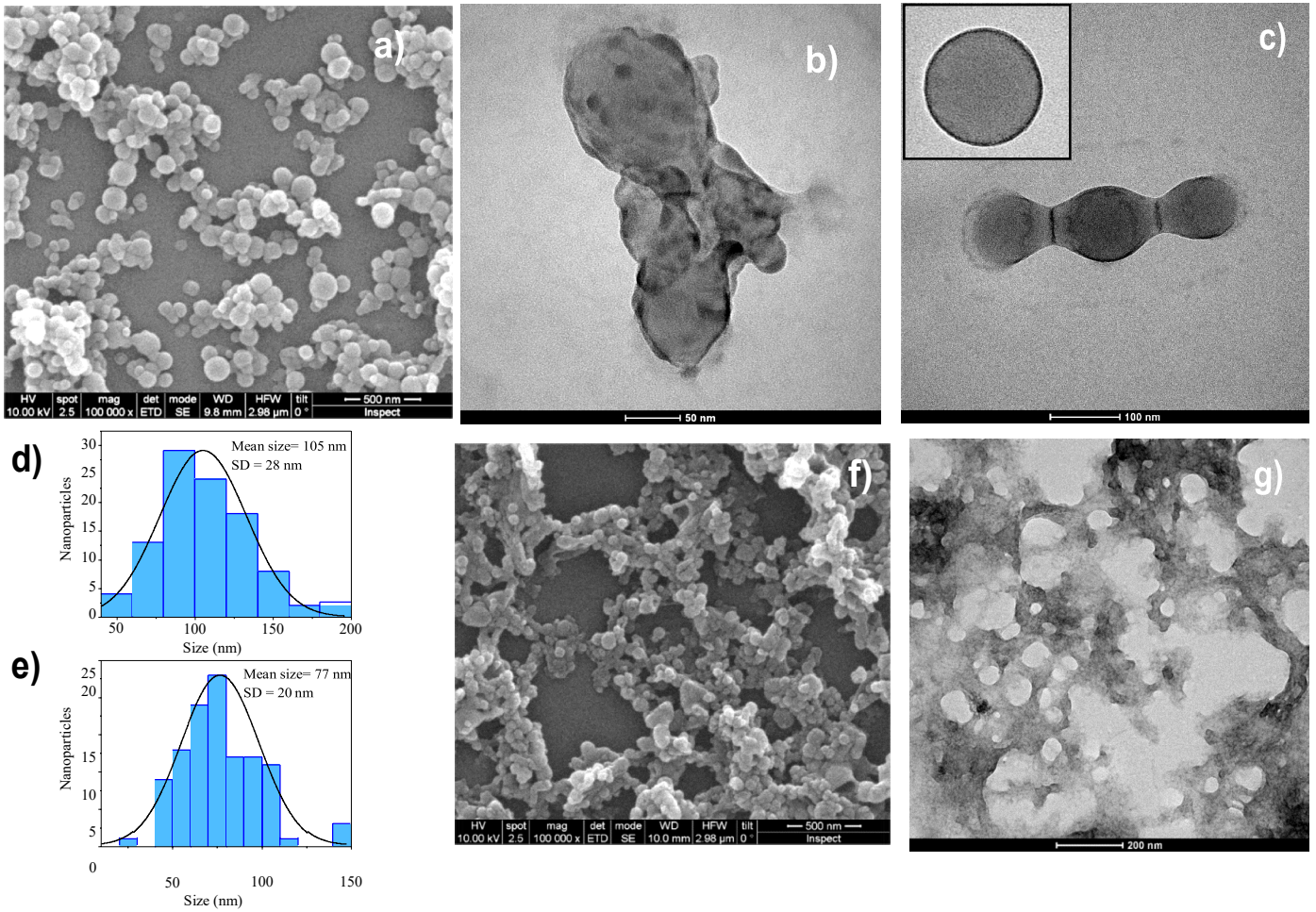

Figure 1 SEM (a) and TEM (b) images of PLGA-colistin nanoparticles obtained by o/w emulsification using 50 mg of colistin. (c) PLGA-colistin nanoparticles obtained by o/w emulsification using 50 mg of colistin after incubation in water with a pH adjusted to 6. (d) Size distribution histogram retrieved from SEM measurements (N=100) of nanoparticles in (a). (e) Histogram of PLGA-PEG-colistin nanoparticles obtained by nanoprecipitation using 9 mg of colistin in the synthesis. SEM (f) and TEM (g) images of PLGA-PEG-colistin nanoparticles obtained by nanoprecipitation using 9 mg of colistin.

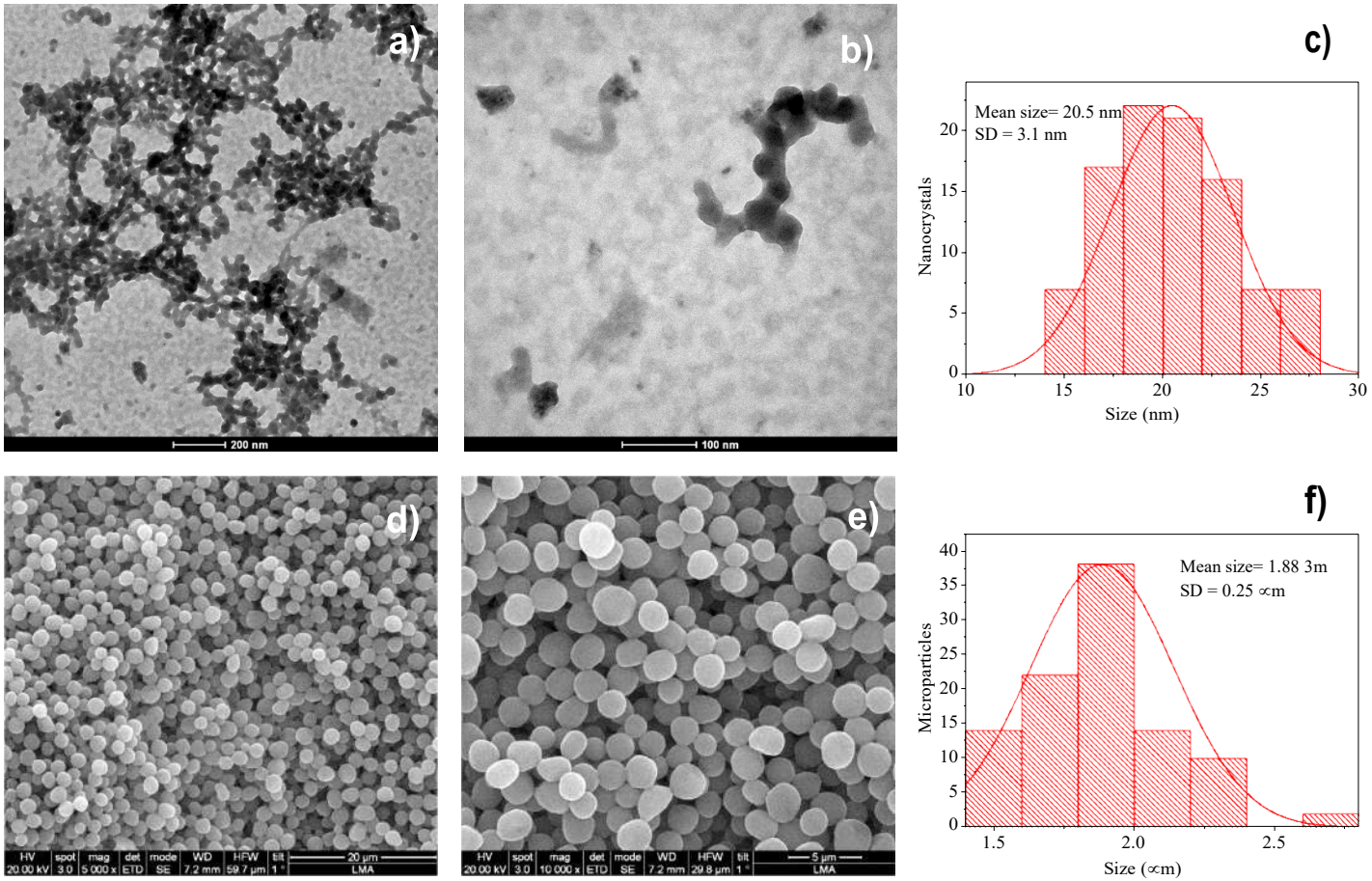

Figure 2 (a) and (b) TEM images of colistin nanocrystals obtained by anti-solvent precipitation technique using 15 mg of colistin. (c) Size distribution histogram retrieved from TEM measurements (N=100) of colistin nanocrystals obtained by anti- solvent precipitation. (d) and (e) SEM images of PLGA-colistin microparticles obtained by electrospraying. (f) Size distribution histogram retrieved from SEM measurements (N=100) of PLGA-colistin microparticles obtained by electrospraying.

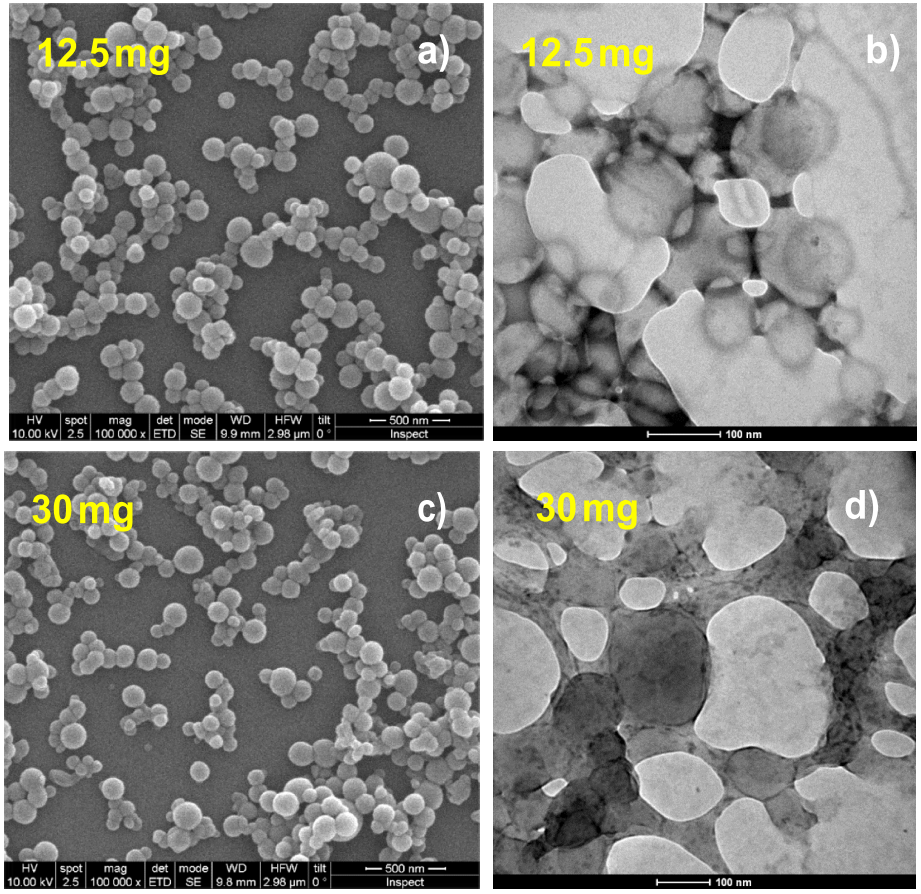

Figure S1 SEM (a) (c) and TEM (b) (d) images of PLGA-colistin nanoparticles obtained by o/w emulsification using 12.5 mg (a) (b) and 30 mg (c) (d) of colistin.

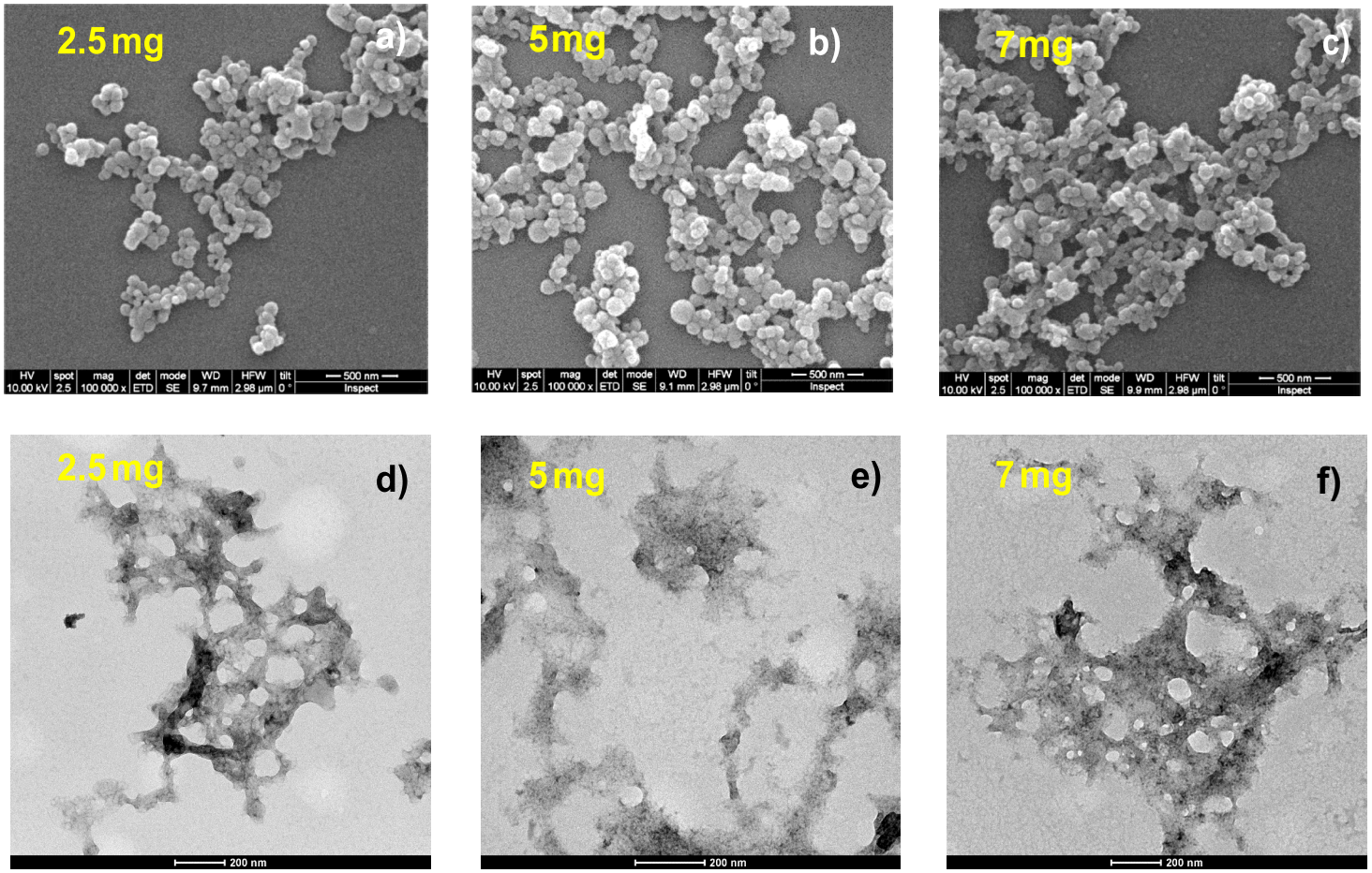

Figure S2 SEM (a) (b) (c) and TEM (d) (e) (f) images of PLGA-PEG-colistin nanoparticles obtained by nanoprecipitation using 2.5 mg (a) (d), 5 mg (b) (e) and 7 mg (c) (f) of colistin.

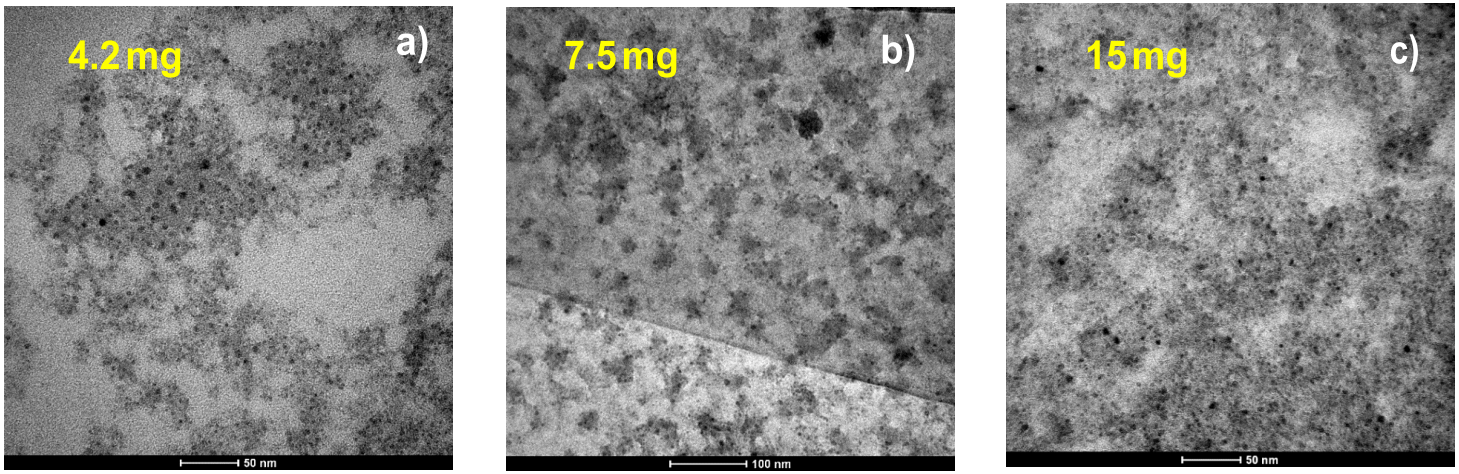

Figure S3 TEM images of colistin nanocrystals obtained by anti-solvent precipitation technique using 4.2 mg (a), 7.5 mg (b) and 12 mg (c) of colistin.

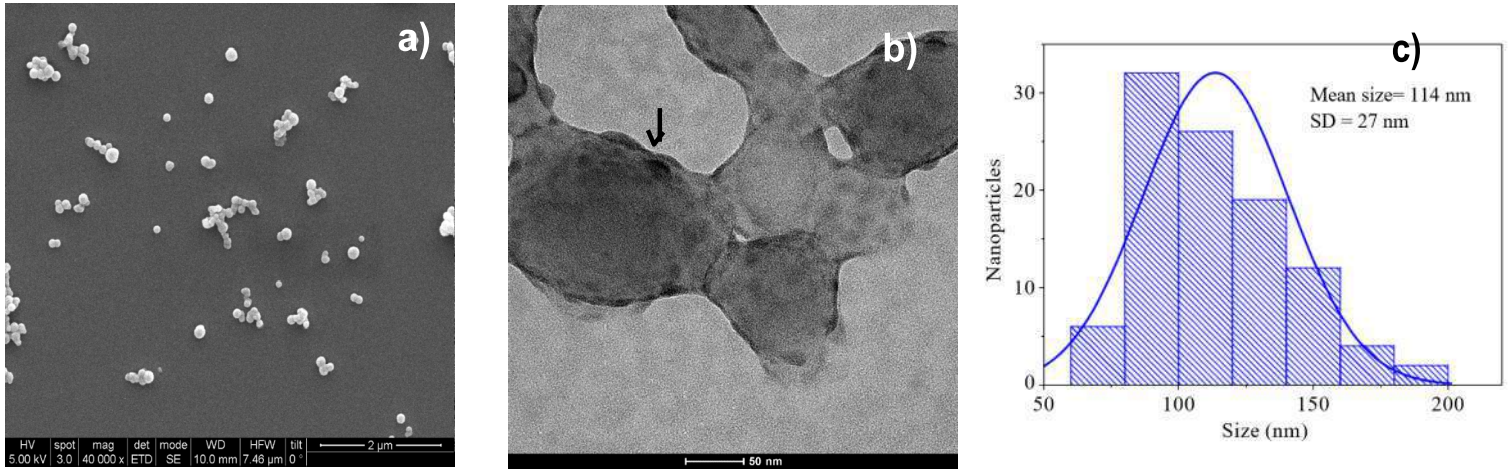

Figure S4 SEM (a) and TEM (b) images of PLGA-colistin nanoparticles obtained by o/w emulsification using 100 mg of CNCs. Arrows indicate dark grey regions located within the particles (indicated with an arrow) attributed to the presence of colistin. (c) Size distribution histogram retrieved from SEM measurements (N=100).

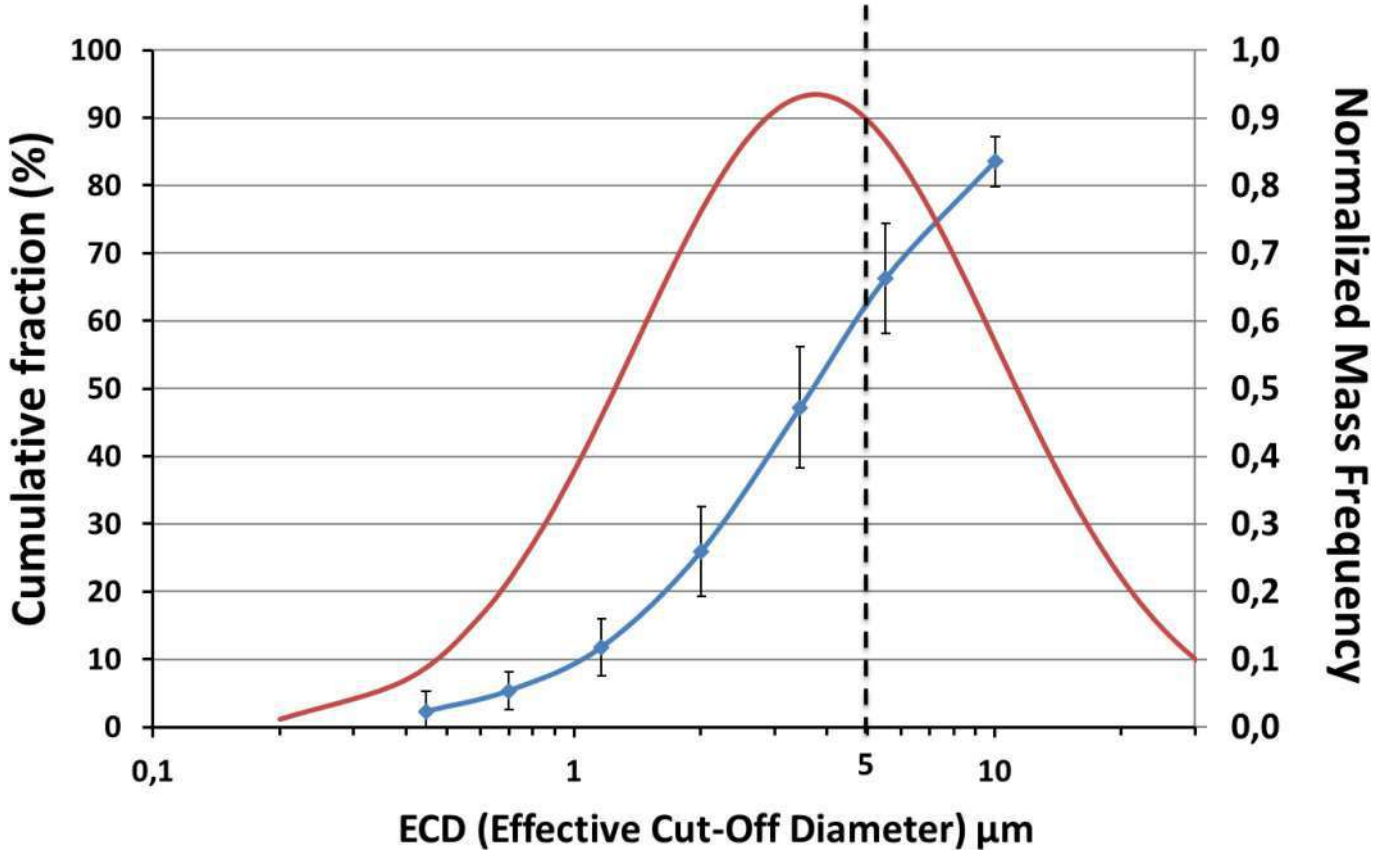

Figure 3 Cascade impactor results for the CNCs. In blue, the cumulative fraction of the particles mass versus Effective cut-off diameter. In red, frequency distribution of the particles mass.

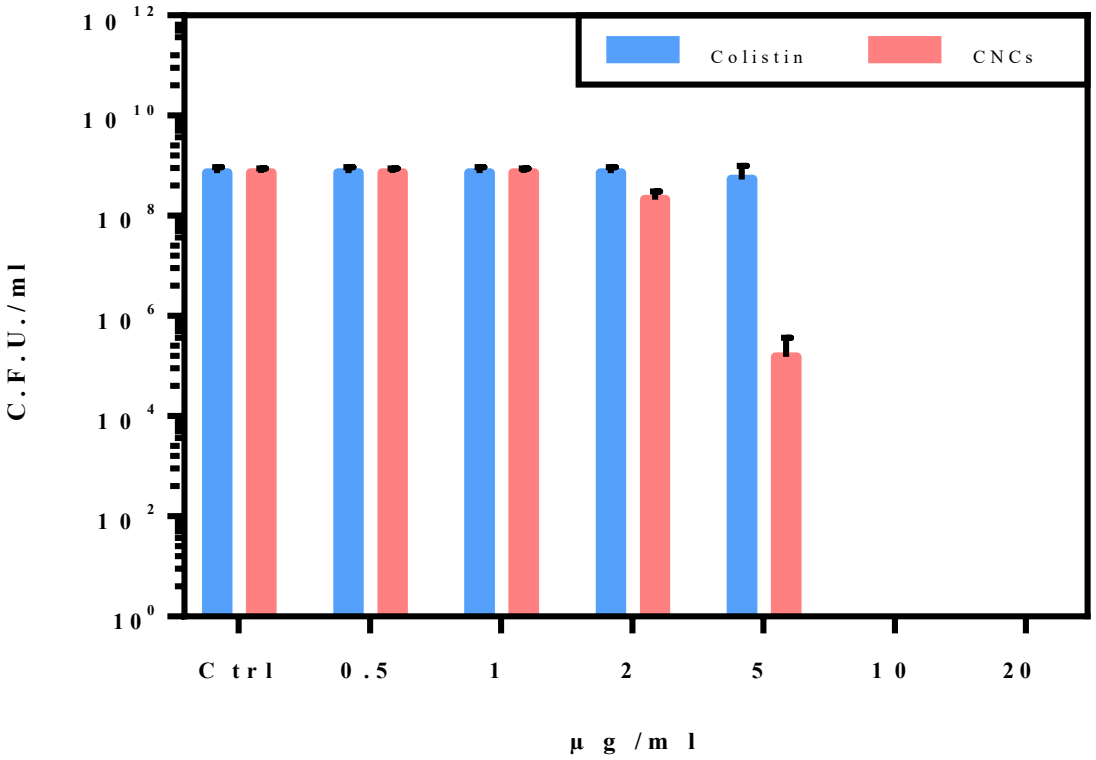

Figure 4 Antimicrobial activity of colistin sulfate and CNCs against PAO1 in alginate-beads biofilm model after 24h. Note that the colistin content in the CNCs is 55.03wt.%.